Biosensors and Bioelectronics 131 (2019) 143–148

Contents lists available at ScienceDirect

Biosensors and Bioelectronics

journal homepage: www.elsevier.com/locate/bios

# Strand displacement amplification-coupled dynamic light scattering method to detect urinary telomerase for non-invasive detection of bladder cancer

Jing Wang[a], Ji Zhang[b], Tingting Li[a], Ruidi Shen[a], Gongke Li[a], Liansheng Ling[a,*]

[a] School of Chemistry, Sun Yat-Sen University, Guangzhou 510275, PR China
[b] State Key Laboratory of Oncology in South China, Collaborative Innovation Center of Cancer Medicine, Sun Yat-Sen University Cancer Center, Guangzhou 510060, PR China

ARTICLE INFO

*Keywords:*
Strand displacement amplification
Dynamic light scattering
Gold nanoparticles
Telomerase activity
Detection
Bladder cancer

ABSTRACT

Despite huge successes achieved by strand displacement amplification (SDA) and gold nanoparticles (AuNPs) in biomolecules sensing, the strategy of combination of SDA and AuNPs-based dynamic light scattering (DLS) for a biomolecule sensing is unexplored. Here we developed a non-invasive, SDA-based DLS method for the diagnosis of bladder cancer by detecting telomerase activity in human urine. In the presence of telomerase, the telomerase substrate (TS) primer was elongated with repeating sequences of (TTAGGG)n, and the resulting product triggers SDA between the hairpin deoxyribonucleic acid (DNA) and the Primer. The SDA product can be recognized by the oligonucleotide-modified AuNPs probes, resulting in DLS measurable AuNPs aggregation. The assay displayed a detection limit of 3 MCF-7 cells with a signal-to-noise ratio of 3 in a dynamic range of 5–1000 cells. The method was simple, reliable and has been successfully applied in the detection of telomerase in urine with good accuracy, selectivity and reproducibility. Moreover, only urine samples from bladder cancer patients induced a significant change in the average hydrodynamic diameter, indicating practical applicability of the method for the non-invasive diagnosis of bladder cancer.

## 1. Introduction

Bladder cancer is one of most common cancer in the world, and its diagnosis mainly relies on cytology and cystoscopy in clinic (Broza et al., 2018; Nelson, 2005). However, these diagnostic tools suffer from some problems, such as the invasiveness, high cost, low sensitivity, rendering them unsuitable for screening bladder cancer at an early stage. To circumvent these limitations, extensive effort has been made in the development of bioanalytical methods for the detection of bladder cancer biomarkers (Konety and Getzenberg, 2001). Among these biomarkers, telomerase in urine has been regarded as a promising biomarker for the prognosis and diagnosis of bladder cancer due to the relevance of its high urinary level to the bladder cancer patients (Sanchini et al., 2004, 2005; Zhuang et al., 2016). In 1994, a telomere repeat amplification protocol (TRAP) assay was developed to detect the telomerase activity of small tissue biopsies (Kim et al., 1994). Since the TRAP assay was first reported, polymerase chain reaction (PCR)-based TRAP has become the most widely used method for telomerase detection, (Herbert et al., 2006; Xu et al., 2010) showing the merit of improved sensitivity. However, strong background from nonspecific amplification and complicated procedures hamper its widespread use. Recently, various PCR-free methods including fluorescence (Lou et al., 2015; Zhang et al., 2016; Zhuang et al., 2017, 2015), chemiluminescence (Li et al., 2011; Wang et al., 2013), colorimetry (Duan et al., 2014; Yang et al., 2017), electrochemistry (Ling et al., 2016) and surface plasmon resonance (Ma et al., 2015) were developed for the detection of telomerase activity. Among these methods, isothermal amplification-based methods were promising for the detection of telomerase activity in terms of sensitivity, ease of manipulation, cost and their performance in complicated biological samples (Zhang et al., 2017).

Strand displacement amplification (SDA) has received great attention since the first report (Hellyer et al., 1999; Zhao et al., 2015), due to its merit of high sensitivity, celerity and generation of specific single-stranded deoxyribonucleic acid (ssDNA) with the assistance of a nicking enzyme (Craw and Balachandran, 2012; Duan et al., 2013; Shi et al., 2014). Moreover, SDA is compatible with different kinds of probes for measurement (Yan et al., 2014), allowing for the development of different types of SDA-based sensors, such as colorimetry (Bi et al., 2013), fluorescence (He et al., 2010; Qu et al., 2018), and chemiluminescence (Chen et al., 2015). Although SDA has gained huge success in developing sensing platform, SDA-based methods for telomerase are few

* Corresponding author.
*E-mail address:* cesllsh@mail.sysu.edu.cn (L. Ling).

https://doi.org/10.1016/j.bios.2019.02.014
Received 24 November 2018; Received in revised form 29 January 2019; Accepted 1 February 2019
Available online 18 February 2019
0956-5663/ 

explored (Ding et al., 2010; Tian et al., 2014; Tian and Weizmann, 2013). For example, Weizmann and co-workers reported a simple exponential isothermal amplification of telomere repeat (EXPIATR) assay for real-time detection of telomerase activity in cell extracts (Tian and Weizmann, 2013). However, fluorescence detection methods were easily susceptible to complicated biological samples and photostability, limiting their practical use (Wang et al., 2016, 2017).

Gold nanoparticles (AuNPs) are widely explored as probes in biomolecule sensing due to its excellent optical property (Saha et al., 2012). AuNPs can not only act as the colorimetric probes (Mirkin et al., 1996), but also serve as resonance light scattering probes (Aslan et al., 2005), electrochemical probes (Yu et al., 2003) and dynamic light scattering (DLS) probes (Dasary et al., 2010). However, it still remains challenging to apply AuNPs probes to detect SDA products, because it is difficult to directly recognize the double-stranded structure of SDA products with DNA-modified AuNPs (DNA-AuNPs) probes. To bridge this gap, He and co-workers established an AuNPs-based SDA sensor by using dual immunoreactions (He et al., 2012); Qi and co-workers developed a colorimetric SDA sensor for platelet-derived growth factor-BB (PDGF-BB) by the use of a nicking enzyme (Zhang et al., 2015). On the other hand, AuNPs-based DLS has become a competitive optical technique for the detection of metal ions (Miao et al., 2012, 2011), proteins (Miao et al., 2014), and DNA (Yin et al., 2014), because its sensitivity is about four orders of magnitude higher than that of AuNPs-based colorimetric methods (Dai et al., 2008). In consideration of the sensitivity of nucleic acid amplification-based methods, the development of DLS sensors based on DNA-AuNPs probes and nucleic acid amplification is also emerging (Liu et al., 2008; Yin et al., 2014), but SDA-based DLS sensor has not been explored.

In this work, inspired by the merits of SDA and DLS, we developed an SDA-coupled DLS method for the detection of telomerase activity. Generally, the generation of ssDNA products in SDA requires the participation of a nicking enzyme, rendering sensing systems complicated and susceptible. We reasoned that the introduction of a C18 spacer into the hairpin DNA and the primer can leave two single-stranded sequences in two ends of SDA products, enabling specific recognition with DNA-AuNPs probes and further DLS measurement.

## 2. Material and methods

### 2.1. Chemicals and reagents

All oligonucleotides, Klenow fragment (exo$^-$) DNA polymerase, RNase inhibitor, 1 × CHAPS lysis buffer and deoxyribonucleoside triphosphates (dNTPs) were purchased from Sangon Biotech Co., Ltd. (Shanghai, China). Human thrombin, platelet-derived growth factor-BB (PDGF-BB) and bovine serum albumin (BSA) were purchased from Sigma-Aldrich (USA). Chloroauric acid ($HAuCl_4{\cdot}4H_2O$) and tris(2-carboxyethyl)phosphine hydrochloride (TCEP) were purchased from Sinopharm Chemical Reagent Co., Ltd. (Shanghai, China). Ultrapure water (18.2 MΩ cm) was obtained from a Milli-Q water purification system (Millipore Co., USA). All reagents were analytically pure and used as received.

### 2.2. Apparatus

The absorption spectra were recorded on a UV-1750 UV–Vis spectrophotometer (Shimadzu, Japan) at room temperature. DLS and zeta potential tests were performed on an EliteSizer nanoparticle/Zeta potentiometer (Anton Paar Ltd., Austria). Transmission Electron Microscopy (TEM) images were obtained on a JEM-3010 transmission electron microscope. The images of gel electrophoresis were scanned on a Gel Image Analysis System (JY02S, Beijing, China).

### 2.3. Telomerase substrate extension

The cell extracts were first diluted to the different number of cells with lysis buffer. Then the solution containing telomerase extract, 1.5 μM telomerase extension (TS) primer, 1.0 mM dNTPs, 0.2 mg mL$^{-1}$ BSA, 0.4 U μL$^{-1}$ RNase inhibitor was incubated at 37 °C for 1.5 h, and further inactivated by heating at 95 °C for 5 min. Then the solution was added with SDA.

### 2.4. SDA of telomerase activity

The hairpin was heated to 95 °C for 5 min and then allowed to cool down to room temperature before use. The experiments were performed in 40 μL solution consisting of a series of elongated TS primer with different telomerase concentrations from 5 cells to 15000 cells, 0.1 μM hairpin, 0.1 μM primer, 3 U Klenow fragment (exo$^-$) DNA polymerase, 100 mM dNTPs, 6% dimethyl sulfoxide (DMSO), 1 mM dithiothreitol (DTT) and 5 mM magnesium chloride ($MgCl_2$) in 50 mM Tris-HCl (pH 8.0) and incubated at 37 °C.

### 2.5. DLS measurements

Probes A and B were first added to the SDA mixture solution, and then DLS was measured after 10 min of incubation at 37 °C. Then the mixed solution was measured by using the DLS technique at 25 °C with a 10 s equilibration time and 90° measurement angle. All sizes reported here were based on the intensity of particle size distributions, and each reported particle size was the average of three times measurements.

## 3. Results and discussion

### 3.1. The principle for the target assay

The strategy for the detection of telomerase activity is illustrated in Fig. 1. The oligonucleotide 5′-AATCCGTCGAGCAGAGTT-3′ is the telomerase extension primer (TS primer), which can be extended in the presence of telomerase and dNTPs. The oligonucleotides 5′-SH-TTTTT TATCACATCA-3′ and 5′-SH-TTTTTTAAGGAGTGT-3′ are designed to modify AuNPs, acting as signal probes A and B, respectively. The oligonucleotide 5′-*ACACTCCTT*-C18 spacer-TCTTGGAC<u>TAACCCTAACCC TAAAAC</u>**TTAGTCCAAGA**-3′ are designed as a hairpin DNA for the system. It contains two parts: the underlined part in the loop is to hybridize with the elongated TS primer; the italic part in the stem is to hybridize with Probe B; and the bold part in the stem is to hybridize with the Primer to induce the SDA. The oligonucleotide 5′-*TGATGT GAT*-C18 spacer-**TCTTGGAC**-3′ is designed as the Primer, which the bold part used to initialize the SDA reaction, while the italic part to hybridize with the Probe A. The C18 spacers in the Primer and hairpin DNA serve as blockers for extension of double-stranded

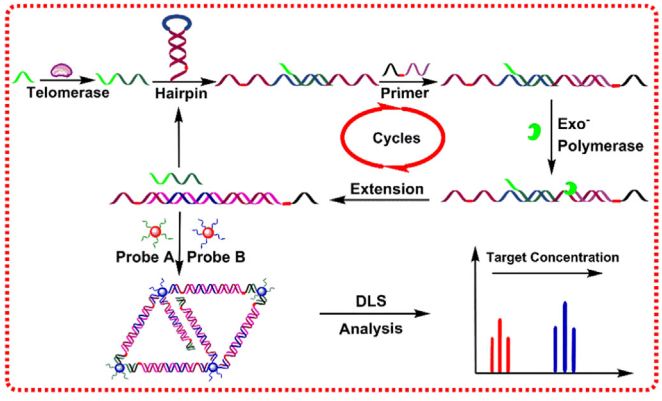


**Fig. 1.** Schematic diagram of telomerase detection strategy.

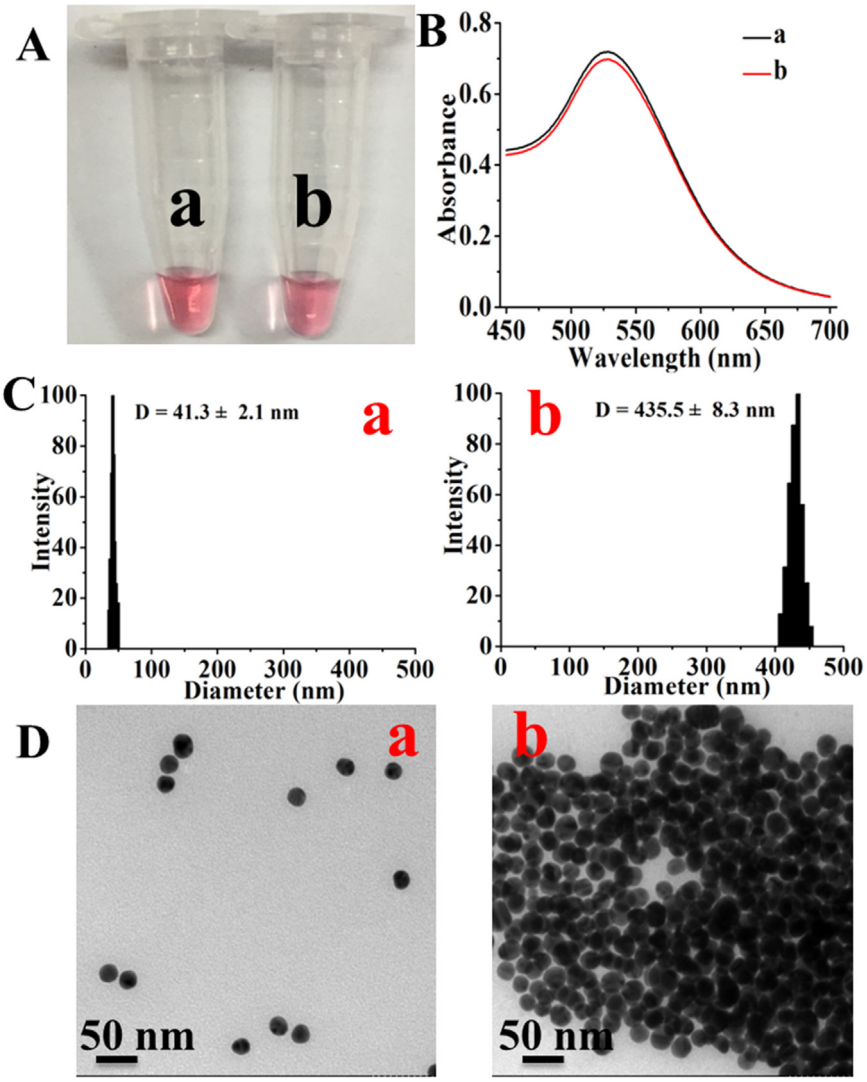


**Fig. 2.** (A) Image of the AuNPs solution. (B) UV–Vis absorption spectra of the SDA-DLS sensing method. (C) DLS of the SDA-DLS sensing method, RSD of (a) is 2.1 while RSD of (b) is 8.3. (D) TEM of the SDA-DLS sensing method: (a) SDA product in the absence of telomerase from 5000 MCF-7 cells; (b) SDA product in the presence of telomerase from 5000 MCF-7 cells.

deoxyribonucleic acid (dsDNA), instead of nicking enzymes to produce ssDNA segments in SDA products.

Upon addition of telomerase, the TS primer is elongated with the repeated sequence of $(TTAGGG)_n$ (green in Fig. 1), and the elongated TS primer hybridizes with the loop of the hairpin DNA, resulting in the opening of the hairpin DNA. Opened hairpin DNA is then recognized by the Primer on its stem sequence, triggering an SDA process in the presence of dNTPs and Klenow fragment ($exo^-$) DNA polymerase. The elongated TS primer will be released during each cycle, enabling it to trigger a new cycle of SDA continually. Because the polymerization of the respective templates will be blocked at C18 spacer, so the SDA product contains free ssDNA segments at both ends. These ssDNA segments can hybridize with the probes A and B, inducing the aggregation of the AuNPs, and further enabling the measurement by DLS technique.

### 3.2. Feasibility of the strategy

To investigate the feasibility of the strategy, UV–Vis absorbance, DLS and TEM and zeta potential measurements were employed. The telomerase was extracted from a human breast carcinoma cell line MCF-7 as a telomerase source. As shown in Fig. 2A, no obvious color change was observed in the absence and presence of telomerase from 5000 MCF-7 cells, which was further confirmed by UV–Vis absorption spectra (Fig. 2B). In contrast, there was a dramatic increase in the DLS signal (Fig. 2C). The hydrodynamic diameter of SDA product was 41.3 nm in the absence of telomerase (Fig. 2Ca), while the average hydrodynamic diameter increased to 435.5 nm in the presence of telomerase from 5000 MCF-7 cells (Fig. 2Cb). The DLS signal change was further verified by TEM images, which showed that the AuNPs were well-dispersed in the absence of telomerase, which they aggregated in the presence of telomerase. A zeta potential measurement experiment was also carried out. The results showed that probes A and B exhibited reduced zeta potential than the AuNPs (−32.4 mV vs −22.6 mV and −30.6 vs −22.6 mV) (Table. S1), lying on the fact DNA were negative charged, and their incorporation on AuNPs may reduce the zeta potential (Su and Kanjanawarut, 2009; Zhang et al., 2013). Furthermore, the presence of telomerase increased the zeta potential, which increased from − 34.1 mV to − 15.7 mV, further indicating the aggregation of probe A, probe B with SDA products through DNA linking. Taken together, these results indicate that the proposed strategy has the ability to measure telomerase activity, and DLS is more highly sensitive than the corresponding colorimetric method, which is sensitive enough to detect the SDA product at low concentrations of telomerase.

The SDA product was also investigated with circular dichroism (CD)

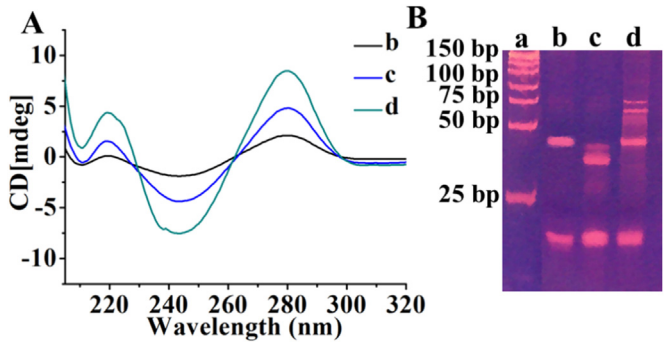


**Fig. 3.** (A) CD spectroscopy of the oligonucleotides in SDA system. (B) polyacrylamide gel electrophoresis image of SDA system; a: the DNA marker; b: TS primer + telomerase; c: TS primer + the Primer + the hairpin DNA; d: TS primer + the Primer + the hairpin DNA + telomerase. All DNA species were at 1 μM; telomerase was extracted from 5000 MCF-7 cells.

spectroscopy and polyacrylamide gel electrophoresis (PAGE). As shown in Fig. 3A, the mixture of TS primer and telomerase displayed a weak positive cotton peak at 278 nm and a negative cotton peak at 248 nm, which were characteristics of ssDNA for TS primer (curve b). Compared to curve b, there were slight increase at 278 nm and 248 nm for the mixture of TS primer, the Primer and the hairpin DNA, ascribed by the dsDNA structure of the hairpin DNA. In contrast, there was a strong increase at 278 nm and 248 nm for the mixture of the TS primer, the Primer, the hairpin DNA and telomerase (curve d), indicating that SDA reaction produced a large amount of dsDNA with the help of telomerase (Wang et al., 2018). These results were further supported by the result of a PAGE test, which showed that the presence of telomerase induced a large number of dsDNA bands (band d). Taken together, this assay can detect telomerase activity in a manner as we expected.

### 3.3. Optimization of assay condition

To improve the assay sensitivity, related parameters which may affect the sensitivity were optimized. Extension time for TS primer in the presence of telomerase was investigated over the range of 30–150 min. As shown in Fig. S2A, the average diameter of the blank kept stable during the whole extension time range, while it increased with the extension time during the range of 30–90 min in the presence of telomerase, reaching a plateau at 90 min, thus 90 min of extension time was used for the following experiments. Extension temperature was then examined, the result showed that the average diameter of the AuNPs increased with the increase of extension temperature within the range of 20–37 °C, achieving a balance at 37 °C (Fig. S2B), thereby 37 °C was selected as the optimal extension temperature. Additionally, the effect of substrate concentration, SDA temperature, the concentration of the DNA-AuNPs probes, time for hybridization between the DNA-AuNPs probes and SDA product were investigated as well. As shown in Figs. S2C-F, 1.0 μM of substrate concentration, 37 °C of SDA temperature, 2.0 nM of the DNA-AuNPs probes and 10 min of hybridization time between the DNA-AuNPs probes and the SDA product were found to be optimal parameters.

### 3.4. Telomerase activity assay by DLS in the buffer

To examine the sensitivity of the assay, the linear relationship between the average diameter of the AuNPs and the telomerase activity was investigated. Under optimal conditions, the average diameter steadily increased with the increase of extracted MCF-7 cell number (Fig. 4A). There existed a good linear relationship between the average diameter of the AuNPs and the MCF-7 cell number within a range of 5–1000 cells, the linear regression equation was $D = 48.10 + 0.35\,n$ (n: cell number, $R^2 = 0.995$), with a detection limit of 3 cells (3δ/slope). The high sensitivity of this method may be attributed to the combination of SDA and AuNPs-based DLS. The sensitivity of our method was also compared with other types of methods for telomerase detection (Table S2).

Selectivity of the proposed method for telomerase activity was investigated using BSA, thrombin and PDGF-BB. As shown in Fig. 4B, the average diameter for telomerase from 5000 MCF-7 cells increased significantly, while the average diameter for 1.0 nM of BSA, thrombin or PDGF-BB remained the same as that of the blank. These results indicated that only the presence of telomerase can trigger the SDA amplification, demonstrating that the proposed method has high selectivity for telomerase activity, which is suitable for further applications. Additionally, the response of the method to bladder cancer cells and human normal cells was investigated. Bladder cancer cells T24 and normal cells HUVEC were chosen, the results showed that the average diameter for T24 cells enhanced significantly, while the diameter for HUVEC cells remained the same as the blank (Fig. S1). These indicated that our method can be capable of detecting telomerase from different kinds of cancer cells, and also can discriminate cancer cells from normal cells, further confirming that the applicability of our method.

### 3.5. Detection of telomerase activity in urine sample

To investigate the feasibility of this assay in complicated biological matrixes, a recovery experiment was conducted in spiked human urine samples. As shown in Table 1, telomerase extracted from the different number of cells was added into the solution containing 10% human urine, the recovery varied from 96.0% to 110.0%, while the relative standard deviation (RSD) varied from 1.7% to 3.2%. These results demonstrated the capability of this method to accurately measure telomerase in biological samples, prompting us to explore its further practical applicability.

Urinary telomerase has been identified as a promising biomarker for the prognosis and diagnosis of bladder cancer (Sanchini et al., 2004, 2005), so we tested whether this assay can be applied to the non-invasive diagnosis of bladder cancer. 21 samples were collected from normal individuals and patients who suffering from bladder cancer, breast cancer, liver cancer, gastric cancer and lung cancer from Sun Yat-Sen University Cancer Center. Urine samples were treated to extract telomerase according to a typical procedure (Liu et al., 2016). The resulted samples were then analyzed by using this assay. As shown in Table 2, the average diameter for the samples from bladder cancer patients increased dramatically to over 210 nm, whereas that for normal individuals or other cancer patients varied around 50 nm. Besides, the zeta potential of the real samples were also determined and shown in Table S1. The zeta potential for bladder cancer samples was much higher than that for normal and other cancer, further indicating the aggregation of probe A, probe B with SDA products. These results indicated that this assay was capable of discriminating bladder cancer patients from normal individuals, even from other types of cancers. Therefore, the proposed method shows great potential in non-invasive specific diagnosis of bladder cancer.

## 4. Conclusions

In conclusion, we proposed first SDA-based DLS sensor to measure telomerase activity for non-invasive diagnosis of bladder cancer. In this work, the introduction of a C18 spacer into the primers and hairpin DNA enabled the existence of two ssDNA segments at two ends of SDA products for the recognition by the DNA-AuNPs probes, avoiding the use of nicking enzymes. Moreover, the combination of the amplification power of SDA and the sensitivity of DLS technique endowed this assay with high sensitivity and selectivity for telomerase activity, which the detection limit reached as low as 3 MCF-7 cells. This assay further demonstrated its applicability in spiked human urine samples, with

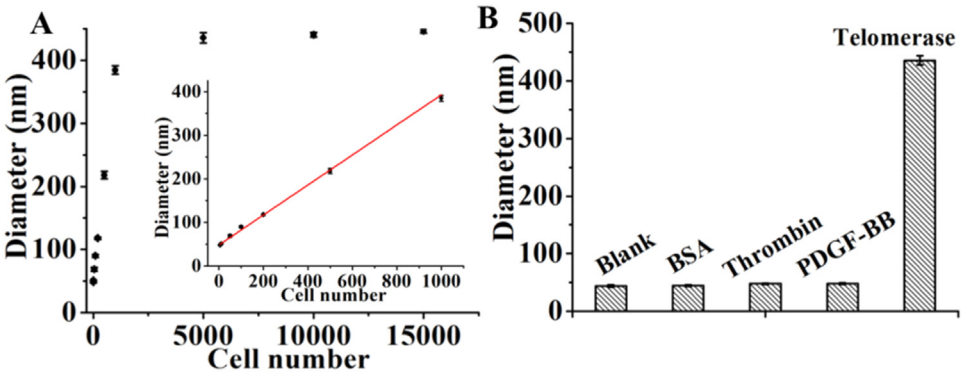


**Fig. 4.** (A) Relationship between the average diameters of AuNPs and the telomerase extracts from different numbers of MCF-7 cells, Inset: the calibration curve versus cell number from 5 to 1000. (B) DLS selectivity of the proposed method for thrombin. The concentration of BSA, thrombin and PDGF-BB is 1.0 nM, respectively. Telomerase was obtained from 5000 MCF-7 cells. Error bars show the standard deviations of three experiments.

**Table 1**
Recoveries of telomerase from the spiked human urine samples.

| Samples | Added number | Found number | Recovery (%) | RSD (%) |
|---|---|---|---|---|
| DLS | 50 | 48 | 96.0 | 2.3 |
| | 100 | 110 | 110.0 | 1.7 |
| | 200 | 207 | 103.5 | 3.2 |
| | 500 | 501 | 100.2 | 2.1 |

**Table 2**
Comparison of the results by clinical diagnosis and the proposed method[a].

| No. | Patient ID | Clinical outcome | Diameter (nm) | Judgement |
|---|---|---|---|---|
| 1 | Normal | Normal | 47.0 ± 2.7 | negative |
| 2 | Normal | Normal | 48.9 ± 3.7 | negative |
| 3 | Normal | Normal | 45.0 ± 5.1 | negative |
| 4 | 0000393109 | Bladder cancer | 211.9 ± 1.3 | positive |
| 5 | 0000393117 | Bladder cancer | 330.1 ± 7.6 | positive |
| 6 | 0000393243 | Bladder cancer | 351.0 ± 6.3 | positive |
| 7 | 0000393218 | Bladder cancer | 368.0 ± 3.1 | positive |
| 8 | 0000392760 | Bladder cancer | 349.2 ± 2.8 | positive |
| 9 | 0000392594 | Bladder cancer | 369.3 ± 0.7 | positive |
| 10 | 0000393190 | Bladder cancer | 454.9 ± 5.7 | positive |
| 11 | 0000394042 | Breast cancer | 48.3 ± 1.5 | negative |
| 12 | 0000394058 | Breast cancer | 49.8 ± 3.3 | negative |
| 13 | 0000393890 | Breast cancer | 52.2 ± 1.3 | negative |
| 14 | 0000395010 | Liver cancer | 50.3 ± 3.6 | negative |
| 15 | 0000395074 | Liver cancer | 54.5 ± 0.97 | negative |
| 16 | 0000394956 | Liver cancer | 56.6 ± 1.9 | negative |
| 17 | 0000394945 | Gastric cancer | 58.3 ± 0.5 | negative |
| 18 | 0000395389 | Gastric cancer | 53.7 ± 3.6 | negative |
| 19 | 0000395358 | Lung cancer | 46.8 ± 1.8 | negative |
| 20 | 0000395018 | Lung cancer | 49.7 ± 4.7 | negative |
| 21 | 0000395265 | Lung cancer | 48.0 ± 2.8 | negative |

[a] Clinical outcomes provided by Sun Yat-Sen University Cancer Center.

satisfactory recoveries ranging from 96.0% to 110.0%. Importantly, the proposed method was successfully applied to detect the telomerase activity in urine from normal individuals and different cancer patients, differentiating bladder cancer patients from other groups. Taken together, this method shows the great potential in the detection of telomerase, serving as a promising non-invasive diagnostic tool to screen bladder cancer in clinical applications.

## CRediT authorship contribution statement

**Jing Wang:** Conceptualization, Methodology, Software, Validation, Formal analysis, Investigation, Data curation, Writing - original draft, Visualization, Project administration. **Ji Zhang:** Resources, Data curation. **Tingting Li:** Validation, Formal analysis. **Ruidi Shen:** Validation, Formal analysis. **Gongke Li:** Supervision, Funding acquisition. **Liansheng Ling:** Conceptualization, Writing - review & editing, Visualization, Supervision, Project administration, Funding acquisition.

## Acknowledgments

This work was supported by the National Natural Science Foundation of China (Grant No. 21375153, 21475153 and 21675178).

## Declaration of interests

None.

## Appendix A. Supporting information

Supplementary data associated with this article can be found in the online version at https://doi.org/10.1016/j.bios.2019.02.014.

## References

Aslan, K., Lakowicz, J.R., Geddes, C.D., 2005. Anal. Chem. 77 (7), 2007–2014.
Bi, S., Cui, Y., Li, L., 2013. Anal. Chim. Acta 760, 69–74.
Broza, Y.Y., Vishinkin, R., Barash, O., Nakhleh, M.K., Haick, H., 2018. Chem. Soc. Rev. 47 (13), 4781–4859.
Chen, A., Gui, G.-F., Zhuo, Y., Chai, Y.-Q., Xiang, Y., Yuan, R., 2015. Anal. Chem. 87 (12), 6328–6334.
Craw, P., Balachandran, W., 2012. Lab Chip 12 (14), 2469–2486.
Dai, Q., Liu, X., Coutts, J., Austin, L., Huo, Q., 2008. J. Am. Chem. Soc. 130 (26), 8138–8139.
Dasary, S.S.R., Senapati, D., Singh, A.K., Anjaneyulu, Y., Yu, H., Ray, P.C., 2010. ACS Appl. Mater. Interfaces 2 (12), 3455–3460.
Ding, C., Li, X., Ge, Y., Zhang, S., 2010. Anal. Chem. 82 (7), 2850–2855.
Duan, R., Wang, B., Zhang, T., Zhang, Z., Xu, S., Chen, Z., Lou, X., Xia, F., 2014. Anal. Chem. 86 (19), 9781–9785.
Duan, R., Zuo, X., Wang, S., Quan, X., Chen, D., Chen, Z., Jiang, L., Fan, C., Xia, F., 2013. J. Am. Chem. Soc. 135 (12), 4604–4607.
He, J.-L., Wu, Z.-S., Zhou, H., Wang, H.-Q., Jiang, J.-H., Shen, G.-L., Yu, R.-Q., 2010. Anal. Chem. 82 (4), 1358–1364.
He, Y., Zeng, K., Zhang, S., Gurung, A.S., Baloda, M., Zhang, X., Liu, G., 2012. Biosens. Bioelectron. 31 (1), 310–315.
Hellyer, T.J., Desjardin, L.E., Teixeira, L., Perkins, M.D., Cave, M.D., Eisenach, K.D., 1999. J. Clin. Microbiol. 37 (3), 518–523.
Herbert, B.-S., Hochreiter, A.E., Wright, W.E., Shay, J.W., 2006. Nat. Protoc. 1 (3), 1583–1590.
Kim, N.W., Piatyszek, M.A., Prowse, K.R., Harley, C.B., West, M.D., Ho, P.L.C., Coviello, G.M., Wright, W.E., Weinrich, S.L., Shay, J.W., 1994. Science 266 (5193), 2011–2015.
Konety, B.R., Getzenberg, R.H., 2001. J. Urol. 165 (2), 600–611.
Li, Y., Li, X., Ji, X., Li, X., 2011. Biosens. Bioelectron. 26 (10), 4095–4098.
Ling, P., Lei, J., Jia, L., Ju, H., 2016. Chem. Commun. 52 (6), 1226–1229.
Liu, X., Dai, Q., Austin, L., Coutts, J., Knowles, G., Zou, J., Chen, H., Huo, Q., 2008. J. Am.

Chem. Soc. 130 (9), 2780–2782.
Liu, X., Wei, M., Liu, Y., Lv, B., Wei, W., Zhang, Y., Liu, S., 2016. Anal. Chem. 88 (16), 8107–8114.
Lou, X., Zhuang, Y., Zuo, X., Jia, Y., Hong, Y., Min, X., Zhang, Z., Xu, X., Liu, N., Xia, F., 2015. Anal. Chem. 87 (13), 6822–6827.
Ma, X., Truong, P.L., Anh, N.H., Sim, S.J., 2015. Biosens. Bioelectron. 67, 59–65.
Miao, X.-M., Ling, L.-S., Shuai, X.-T., 2012. Anal. Biochem. 421 (2), 582–586.
Miao, X., Ling, L., Shuai, X., 2011. Chem. Commun. 47 (14), 4192–4194.
Miao, X., Zou, S., Zhang, H., Ling, L., 2014. Sens. Actuators B-Chem. 191, 396–400.
Mirkin, C.A., Letsinger, R.L., Mucic, R.C., Storhoff, J.J., 1996. Nature 382 (6592), 607–609.
Nelson, R., 2005. Lancet Oncol. 6 (12), 927.
Qu, X., Jin, H., Liu, Y., Sun, Q., 2018. Anal. Chem. 90 (5), 3482–3489.
Saha, K., Agasti, S.S., Kim, C., Li, X., Rotello, V.M., 2012. Chem. Rev. 112 (5), 2739–2779.
Sanchini, M.A., Bravaccini, S., Medri, L., Gunelli, R., Nanni, O., Monti, F., Baccarani, P.C., Ravaioli, A., Bercovich, E., Amadori, D., 2004. Neoplasia 6 (3), 234–239.
Sanchini, M.A., Gunelli, R., Nanni, O., Bravaccini, S., Fabbri, C., Sermasi, A., Bercovich, E., Ravaioli, A., Amadori, D., Calistri, D., 2005. Jama 294 (16), 2052–2056.
Shi, C., Liu, Q., Ma, C., Zhong, W., 2014. Anal. Chem. 86 (1), 336–339.
Su, X., Kanjanawarut, R., 2009. ACS Nano 3 (9), 2751–2759.
Tian, L., Cronin, T.M., Weizmann, Y., 2014. Chem. Sci. 5 (11), 4153–4162.
Tian, L., Weizmann, Y., 2013. J. Am. Chem. Soc. 135 (5), 1661–1664.
Wang, J., Li, H., Li, T., Ling, L., 2018. Microchim. Acta 185 (9) (410–410).
Wang, L., Zhang, Y., Zhang, C., 2013. Anal. Chem. 85 (23), 11509–11517.
Wang, W., Mao, Z., Wang, M., Liu, L.-J., Kwong, D.W.J., Leung, C.-H., Ma, D.-L., 2016. Chem. Commun. 52 (18), 3611–3614.
Wang, W., Vellaisamy, K., Li, G., Wu, C., Ko, C.-N., Leung, C.-H., Ma, D.-L., 2017. Anal. Chem. 89 (21), 11679–11684.
Xu, T., Lu, B., Tai, Y.-C., Goldkorn, A., 2010. Cancer Res. 70 (16), 6420–6426.
Yan, L., Zhou, J., Zheng, Y., Gamson, A.S., Roembke, B.T., Nakayama, S., Sintim, H.O., 2014. Mol. Biosyst. 10 (5), 970–1003.
Yang, H., Liu, A., Wei, M., Liu, Y., Lv, B., Wei, W., Zhang, Y., Liu, S., 2017. Anal. Chem. 89 (22), 12094–12100.
Yin, H., Huang, X., Ma, W., Xu, L., Zhu, S., Kuang, H., Xu, C., 2014. Biosens. Bioelectron. 52, 8–12.
Yu, A.M., Liang, Z.J., Cho, J., Caruso, F., 2003. Nano Lett. 3 (9), 1203–1207.
Zhang, H., Li, F., Chen, H., Ma, Y., Qi, S., Chen, X., Zhou, L., 2015. Sens. Actuators B-Chem. 207, 748–755.
Zhang, X., Cheng, R., Shi, Z., Jin, Y., 2016. Biosens. Bioelectron. 75, 101–107.
Zhang, X., Gouriye, T., Go¨eken, K., Servos, M.R., Gill, R., Liu, J., 2013. J. Phys. Chem. C 117 (30), 15677–15684.
Zhang, X., Lou, X., Xia, F., 2017. Theranostics 7 (7), 1847–1862.
Zhao, Y., Chen, F., Li, Q., Wang, L., Fan, C., 2015. Chem. Rev. 115 (22), 12491–12545.
Zhuang, Y., Huang, F., Xu, Q., Zhang, M., Lou, X., Xia, F., 2016. Anal. Chem. 88 (6), 3289–3294.
Zhuang, Y., Shang, C., Lou, X., Xia, F., 2017. Anal. Chem. 89 (3), 2073–2079.
Zhuang, Y., Zhang, M., Chen, B., Duan, R., Min, X., Zhang, Z., Zheng, F., Liang, H., Zhao, Z., Lou, X., 2015. Anal. Chem. 87 (18), 9487–9493.